Quantum and Classical Thermal Correlations in Spin-1 Heisenberg Chain with Alternating Single-Ion Anisotropy

H. Bahmani[1] · G. Najarbashi[1] · B. Tarighi[1] · A. Tavana[1]

Abstract

In the present paper, we study the quantum phase transition in a spin-1 Heisenberg model with two and three particles by using pairwise classical and quantum thermal correlations and entanglement measures, that is, the generalized concurrence and the negativity at finite temperatures. We have used thermodynamic functions of particle number and particle susceptibility to characterize the thermodynamical behavior. The pairwise correlations are derived based on a necessary and sufficient condition for the zero-discord state. We obtain analytical results for the coherence-vector representation of a bipartite state. Using the exact diagonalization technique, we demonstrate that the quantum critical points, detected by the particle number and the particle susceptibility, are ultimately in close correspondence to that of thermal pairwise correlations and entanglement measures.

Keywords Thermal correlations · Quantum phase transition · Spin chains

1 Introduction

Correlations are a major concept in many-body physics, and they play an important role in quantum information and quantum computation sciences. In fact, when the correlation between constituents of a many-body system changes, usually the physical properties of the system are drastically impressed. The study of entanglement is one of the major goals of quantum information science and has wide application in quantum computation, teleportation and cryptography [1]. Entanglement is a kind of correlation which does not exist in a classical system. Recently, an extended kind of entanglement, that is, thermal entanglement, [2–11], has been introduced and studied, extensively, in spin chain models. The connection between the quantum information theory and the condensed matter physics is provided by studying the thermal entanglements, ground state entanglements [12, 13] and the relationship [14, 15]

✉ G. Najarbashi
najarbashi@uma.ac.ir

1   Department of Physics, University of Mohaghegh Ardabili, Ardabil 179, Iran

between them and QPTs [16]. However, recent studies show that entanglement is not the only kind of nonclassical correlation and there exist other nonclassical correlations that cannot be captured by entanglement measures [17, 18]. For instance, quantum discord (QD), an information-theoretic measure originally introduced by Olivier and Zurek [17] and by Henderson and Vedral [19], has gained special attention, recently. QD is defined as the minimum difference between mutual information in a quantum system and its classical counterpart. Such a quantum correlation is more general than entanglement because it is capable to measure the quantum correlations of mixed separable states that cannot be captured by investigating the entanglement.

QPT occurs when the ground state of a quantum system acquires critical changes because of quantum fluctuations. As quantum critical phenomena, QPTs are accessible by varying some parameters of the system, for example, external magnetic field or the coupling constant, at absolute zero temperature [16]. However, in order to be able to detect QPT, one has to work at sufficiently low but finite temperatures where the quantum nature of the QPTs is not negligible. Quantum entanglement usually reveals the existence of quantum and classical correlations among the constituents of a system, in the sense that entanglement satisfies the properties of QPT close to quantum critical points via nonanalyticities in the ground state energy [15, 20].

Recently, many studies are devoted to explore the relation between quantum correlations, quantified by QD and QPT. In Ref [21], it is shown that both quantum discord and classical correlations are effective tools in detecting QPTs. More generally, recently it has been verified that several correlation measures can detect the critical points of QPT in quantum critical spin systems [22–24].

According to Haldane's prediction, the one-dimensional spin-1 Heisenberg model has a spin gap, in contrast to the spin-1/2 case [25]. Some quasi-one-dimensional Haldane chains have, already, been investigated which show a magnetic gap in the excitation spectra. Haldane states are destroyed by different types of perturbations. For example, single-ion anisotropy can lead to a long-range order in a quantum disordered magnet [26]. For large positive single-site anisotropy interaction, the Haldane ground state changes into a large-D state without any obvious magnetic order. While, for large negative single site anisotropy, D, the Haldane state changes into the Neel state [27]. Hence, tuning the value of the parameter D can induce phase transitions. Tzeng et al. [28] have investigated the scaling relation of the fidelity susceptibility and the entanglement entropy for the spin-1 XXZ spin chains, with a single-site anisotropy term, by means of a density matrix renormalization group technique. Ren et al. [26] have evaluated the ground state fidelity susceptibility, the entanglement entropy and the Schmidt gap in 1D spin-1 XXZ chains, with alternating single-site anisotropy.

In this work, we investigate pairwise correlations in a spin-1 Heisenberg model in the presence of an alternating single-ion anisotropy term for two and three particles. Based on a necessary and sufficient condition for zero-discord states in the coherence-vector representation of density matrices [29], we use a measure for classical, nonclassical and total amount of correlations. On the other hand, we use the generalized concurrence [30–37] and the negativity [38–40] as measures of entanglement and also particle number and particle susceptibility as the thermodynamic functions to detect

QPTs. We demonstrate that pairwise correlations, measures of entanglement and thermodynamic functions yield the same results for the critical points of QPT. The paper is organized as follows. In Sect. 2, we review the concepts of classical, quantum and total amount of correlations. In Sect. 3, we introduce the system Hamiltonian, thermal states, entanglement measures and thermodynamic functions. In Sect. 4, we investigate the role of model parameters, for example, anisotropic spin–spin interaction, single-ion anisotropy and temperature, in the entanglement measures, pairwise correlation functions and thermodynamic functions for anti-ferromagnetic and ferromagnetic couplings for the two-spin-1 case. In Sect. 5, the same procedure is performed for the three-spin-1 system. The conclusions are drawn in Sect. 6.

2 Correlation Measures

Based on a necessary and sufficient condition for a zero-discord state, Zhou et al. [29] proposed a measure of quantum, classical and total amount of correlations in bipartite states. The general form of the density matrix of a bipartite state, ρ_{AB}, of Hamiltonian H_{AB} in coherence vector representation is

$$
\begin{aligned}
\rho_{AB} = {} & \frac{1}{d_A d_B} I_A \otimes I_B + \frac{1}{2 d_B} \sum_{i=1}^{d_A^2-1} \lambda_{Ai} \big(\hat{\lambda}_{Ai} \otimes I_B \big) \\
& + \frac{1}{2 d_A} \sum_{i=1}^{d_B^2-1} \lambda_{Bi} \big(I_A \otimes \hat{\lambda}_{Bi} \big) + \frac{1}{4} \sum_{i=1}^{d_A^2-1} \sum_{j=1}^{d_B^2-1} K_{ij} \big(\hat{\lambda}_{Ai} \otimes \hat{\lambda}_{Bj} \big),
\end{aligned}
\tag{1}
$$

where the two components of the local Bloch vectors λ_A, λ_B and the second-order correlation tensor K_{ij} are defined as

$$
\begin{aligned}
\lambda_{Ai} &= tr\big(\rho_{AB} \hat{\lambda}_{Ai} \otimes I_B \big), \\
\lambda_{Bi} &= tr\big(\rho_{AB} I_A \otimes \hat{\lambda}_{Bi} \big), \\
K_{ij} &= tr\big(\rho_{AB} \hat{\lambda}_{Ai} \otimes \hat{\lambda}_{Bj} \big),
\end{aligned}
\tag{2}
$$

Here, I is the identity operator and $\hat{\lambda}_{\alpha i} (\alpha = A, B)$ denote the generators of the $SU(N)$ with $i = 1, 2 ..., N^2 - 1$. The generators satisfy the properties:

$$
\hat{\lambda}_i^\dagger = \hat{\lambda}_i, \qquad tr\big(\hat{\lambda}_i \big) = 0, \qquad tr\big(\hat{\lambda}_i \hat{\lambda}_j \big) = 2\delta_{ij}.
\tag{3}
$$

For the particular case where our model is the spin-1 Heisenberg chain, the explicit form of the $SU(3)$ generators are

$$\lambda_1 = \begin{pmatrix} 0 & 1 & 0 \\ 1 & 0 & 0 \\ 0 & 0 & 0 \end{pmatrix}, \quad \lambda_2 = \begin{pmatrix} 0 & -i & 0 \\ i & 0 & 0 \\ 0 & 0 & 0 \end{pmatrix}, \quad \lambda_3 = \begin{pmatrix} 1 & 0 & 0 \\ 0 & -1 & 0 \\ 0 & 0 & 0 \end{pmatrix}, \quad \lambda_4 = \begin{pmatrix} 0 & 0 & 1 \\ 0 & 0 & 0 \\ 1 & 0 & 0 \end{pmatrix},$$

$$\lambda_5 = \begin{pmatrix} 0 & 0 & -i \\ 0 & 0 & 0 \\ i & 0 & 0 \end{pmatrix}, \quad \lambda_6 = \begin{pmatrix} 0 & 0 & 0 \\ 0 & 0 & 1 \\ 0 & 1 & 0 \end{pmatrix}, \quad \lambda_7 = \begin{pmatrix} 0 & 0 & 0 \\ 0 & 0 & -i \\ 0 & i & 0 \end{pmatrix}, \quad \lambda_8 = \frac{1}{\sqrt{3}}\begin{pmatrix} 1 & 0 & 0 \\ 0 & 1 & 0 \\ 0 & 0 & -2 \end{pmatrix}.$$

$$\tag{4}$$

According to theorem 2 in Ref. [29] and the above bipartite quantum states, the measure of the classical, nonclassical and total amount of correlations for any bipartite state, ρ_{AB}, can be defined as

$$\tau\left(\rho_{AB}\right) = \frac{1}{4}\sum_{i=1}^{d_A^2-1}|\Lambda_i|, \qquad C\left(\rho_{AB}\right) = \frac{1}{4}\sum_{i=1}^{d_A-1}|\Lambda_i|, \qquad Q\left(\rho_{AB}\right) = \frac{1}{4}\sum_{i=d_A}^{d_A^2-1}|\Lambda_i|, \tag{5}$$

where Λ_is are obtained by diagonalizing the criterion matrix $\mathbf{\Lambda} = \mathbf{K}\mathbf{K}^T - \lambda_B^2 \lambda_A \lambda_A^T$, in descending order. In the next section, we introduce the entanglement measures and thermodynamic functions in detail.

3 Model and Method

The purpose of this study is to show how classical, quantum and total amount of correlations do coincide with thermodynamic functions in revealing critical points of a system, through a few examples. The Hamiltonian describing the one-dimensional spin-1 XXZ chain with alternating single-ion anisotropy can be written as follows:

$$H = \sum_{i=1}^{N} J\left(S_i^x S_{i+1}^x + S_i^y S_{i+1}^y + \Delta S_i^z S_{i+1}^z\right) + (-1)^i D\left(S_i^z\right)^2, \tag{6}$$

where $S_i^\alpha (\alpha = x, y, z)$ denote the components of $\mathbf{S}$, the spin operator vector on the site i and N is the total number of sites. We assume the periodic boundary condition, namely, $\mathbf{S}_{N+1} \equiv \mathbf{S}_1$. The first term is the exchange interaction in which J can take two values, ± 1. The parameters Δ and D denote anisotropic spin–spin interaction and single-ion anisotropy, respectively. The sum over sites with $\left(S_i^z\right)^2$ can be expressed as spin concentration (particle number)

$$\sum_{i=1}^{N}\left(S_i^z\right)^2 = P - P_0, \tag{7}$$

where P_0 is the number of sites with $S_i^z = 0$ [41].

In the canonical ensemble, the thermal equilibrium state is given by the Gibb's density operator, $\rho(T) = \frac{e^{-\beta H}}{Z} = \sum_i \frac{e^{-\beta E_i}}{Z}|\psi_i\rangle\langle\psi_i|$, where $Z = Tr(e^{-\beta H}) = \sum_i e^{-\beta E_i}$, is the partition function, E_i are the energy eigenvalues, $\beta = \frac{1}{k_B T}$ and k_B is Boltzmann's constant which is assumed to be unity.

The concept of concurrence which was originally proposed by Hill and Wootters for qubit states [42–45] is one of the well-known bipartite entanglement measures which can be used to quantify the amount of entanglement for arbitrary finite-dimensional bipartite as well as multipartite pure and mixed states [31, 46].

For any arbitrary bipartite state, the generalized concurrence [36] can be defined as follows:

$$|\mathbf{C}|^2 = \sum_{\alpha\beta} C_{\alpha\beta}^2, \tag{8}$$

where $C_{\alpha\beta}$ are the components of the concurrence vector $\mathbf{C}$, defined as follows:

$$C_{\alpha\beta}(\rho) = \max\{0, 2\max(\lambda_i^{\alpha\beta}) - \sum_i \lambda_i^{\alpha\beta}\}, \tag{9}$$

where $\lambda_i^{\alpha\beta}$, with $i = 1...4$ are the square roots of the eigenvalues of the matrix $\rho(L_\alpha \otimes L_\beta)\rho^*(L_\alpha \otimes L_\beta)$, and $L_\alpha(\alpha = 1, ..., \frac{d_1(d_1-1)}{2})$ and $L_\beta(\beta = 1, ..., \frac{d_2(d_2-1)}{2})$ are the generators of the $SO(d_1)$ and the $SO(d_2)$, respectively. Here, ρ^* denotes the complex conjugate of the density matrix ρ.

Another well-accepted entanglement measure is the negativity, which is based on the positive partial transposition (PPT) criterion [38, 47]. Negativity is considered as a quantitative version of Peres' criterion for separability, which states that an arbitrary bipartite state, ρ_{AB}, of $H_A \otimes H_B$ is entangled if the matrix obtained by partial transposition with respect to A or B subsystem, ρ_{AB}, has at least one negative eigenvalue.

Comparing with the concurrence, calculation of the negativity is in general easier than the concurrence of mixed states, since it does not need the convex-roof extension. The value of negativity, corresponding to either a pure or a mixed bipartite state, ρ_{AB}, can be defined as follows:

$$Ne = \sum_i |\mu_i|, \tag{10}$$

where μ_is are the negative eigenvalues of ρ^{T_2}, where T_2 denotes the partial transpose with respect to the second subsystem. If $Ne > 0$, the state is entangled. In describing the thermodynamical nature of the system, we use the response of the thermodynamical potential with respect to D, which is as follows

$$P = \langle (S^z)^2 \rangle = -\frac{\partial F}{\partial D}, \tag{11}$$

where the expectation value is taken with respect to the thermal density matrix and $F = -T \ln Z$ is the free energy. We also define the particle susceptibility as [41]

$$\chi_D = \frac{\partial P}{\partial D}. \tag{12}$$

In what follows, we examine two separate cases of two and three particle systems.

4 Two Particle Systems

In this section, the Hamiltonian of the two-particle system is given by the following:

$$H_2 = J\left(S_1^x S_2^x + S_1^y S_2^y + \Delta S_1^z S_2^z\right) - D\left(S_1^z\right)^2 + D\left(S_2^z\right)^2, \tag{13}$$

Here, by diagonalizing the Hamiltonian matrix (13), we obtain the thermal density matrix and the above-mentioned thermodynamic functions. In the following section, we study the behavior of the pairwise correlations, entanglement measures and also particle number and particle susceptibility at low and high temperatures for two ferromagnetic, that is $J = -1$, and anti-ferromagnetic, that is $J = 1$, cases in more detail. Figure 1 shows the generalized concurrence and the negativity (Fig. 1a), the total amount of correlation, classical correlation and quantum correlation (Fig. 1b)

(a)

(b)

(c)
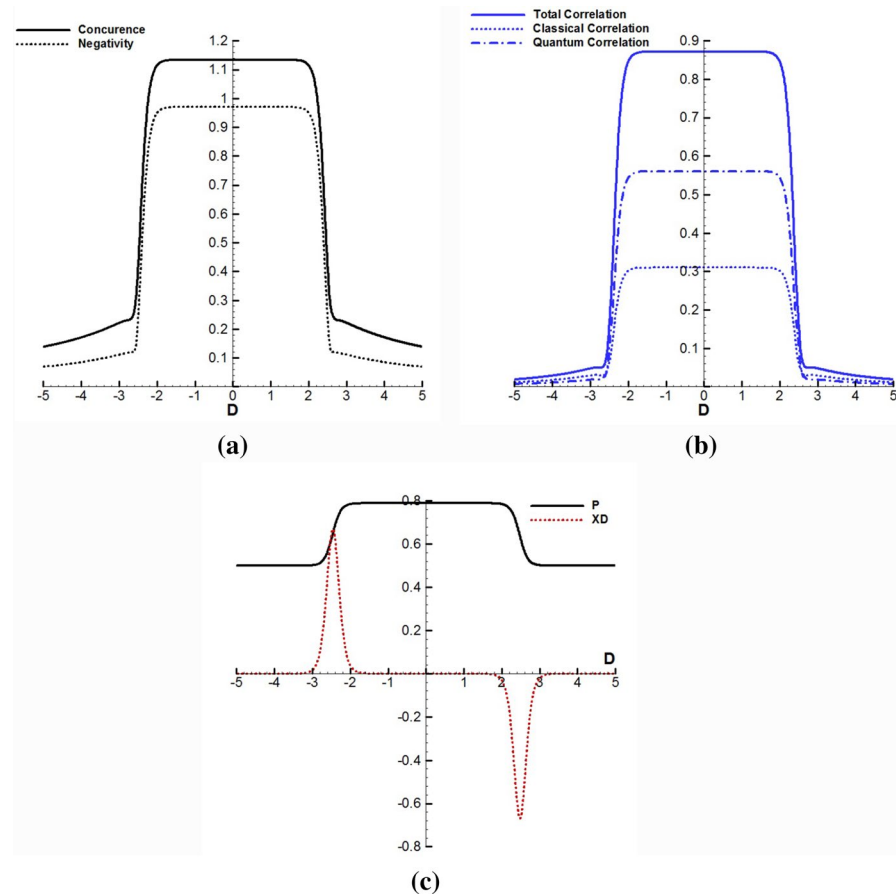
Fig. 1 (Color figure online) Generalized concurrence (solid), negativity (dotted) (**a**), total correlation (solid), classical correlation (dotted) and quantum correlation (dashed) (**b**) and particle number (solid) and particle susceptibility (dotted) (**c**) versus D for $J = 1$ and $\Delta = 2$ at $T = 0.1$

and particle number and particle susceptibility (Fig. 1c) versus D, for the anti-ferromagnetic case, $J = 1$, and $\Delta = 2$ at $T = 0.1$. As depicted in the figure, all the functions yield similar critical points at $D \simeq \pm 2.48$. Within the range specified by $-2.48 < D < 2.48$, classical correlations are smaller than quantum correlations, whereas outside of this range classical correlations are larger than classical correlations. Except for the particle number, all other functions vanish for large D values. Also, except for the particle susceptibility, the other functions peak in the interval $D \in (-2.48, 2.48)$.

Here, we investigate the behavior of entanglement measures, pairwise correlations and thermodynamic functions, P, and χ_D in the ferromagnetic case, that is $J = -1$, when $\Delta = 2$ at $T = 0.1$, as represented in Fig. 2. In this case, the critical points happen at $D \simeq \pm 1.5$. In contrast to the $J = 1$ case, the amount of classical correlations is larger than the quantum correlations so that the classical
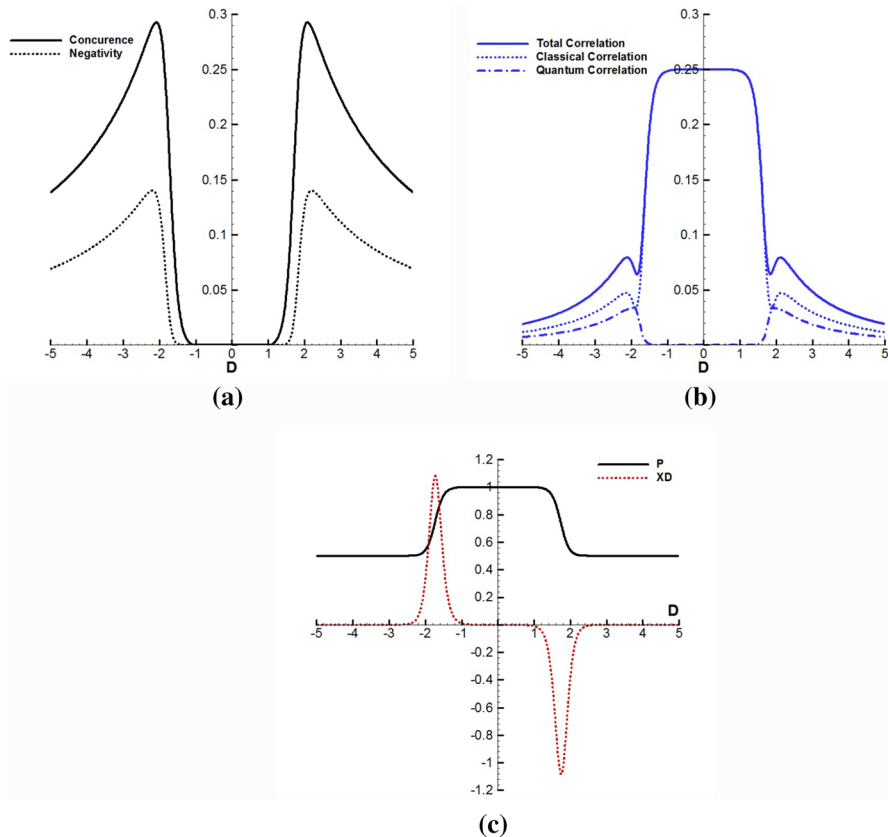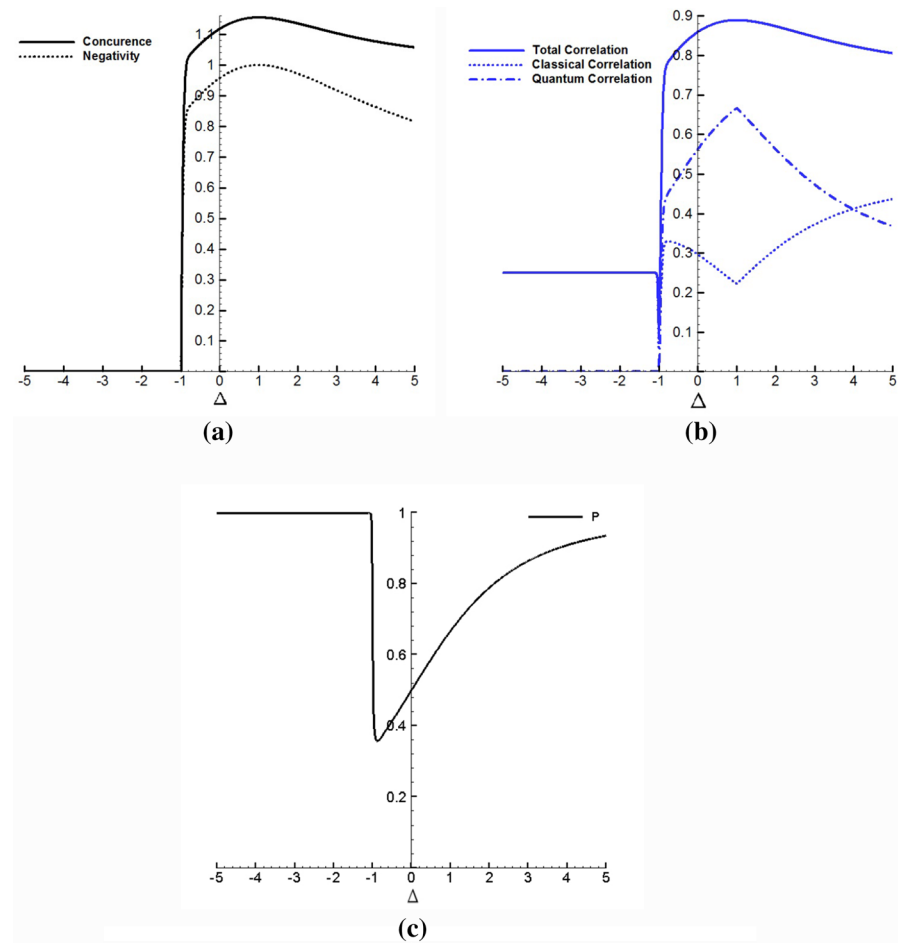

(a)

(b)

(c)

Fig. 2 (Color figure online) Generalized concurrence (solid), negativity (dotted) (**a**), total correlation (solid), classical correlation (dotted) and quantum correlation (dashed) (**b**) and particle number (solid) and particle susceptibility (dotted) (**c**) versus D for $J = -1$ and $\Delta = 2$ at $T = 0.1$

correlations get their maximum value while quantum correlations become zero in the interval $D \in (-1.5, 1.5)$.

Let us now study the effect of parameter Δ when $J = 1$ and $D = 0$ at $T = 0.01$. Looking at Fig. 3, we observe that all functions display a critical point at $\Delta = -1$. Note that in the limit of large positive and large negative values of Δ, all functions become constants with different values. For $\Delta > -1$, quantum correlations can be larger or smaller than classical correlations depending on the Δ parameter. On the other hand, for $\Delta < -1$, entanglement and quantum correlations become zero while the value of classical correlations coincide with total correlations. The results for $J = -1$ are symmetric with respect to $J = 1$ in the sense that for $J = -1$,

Fig. 3 (Color figure online) Generalized concurrence (solid), negativity (dotted) (**a**), total correlation (solid), classical correlation (dotted) and quantum correlation (dashed) (**b**) and particle number (**c**) versus Δ for $J = 1$ and $D = 0$ at $T = 0.01$

the critical point occur at $\Delta = 1$ and the behavior of system for $\Delta > 1$ and $\Delta < 1$ is similar to $\Delta < -1$ and $\Delta > -1$ in the former case, respectively.

The effect of parameter Δ when $J = D = 1$ at $T = 0.01$ is shown in Fig. 4. The same argument as above can be applied to the $D = 1$ case, except for the two critical points corresponding to $\Delta = -1.5$ and $\Delta = 0$, found for the $D = 1$ case. For $J = -1$, the system behaves as symmetric with respect to $J = 1$ in the sense that the critical points are located at $\Delta = 0$ and $\Delta = 1.5$. Let us now look at the behavior of the system in the limit of high temperatures. As temperature is increased, the physical properties of the system will change. As shown in Fig. 5, the variations of all functions with respect to D for $J = 1$, $\Delta = 2$ and $T = 1$, are smooth compared to the low-temperature results, and there is no sharp behavior change in this case. We note that at the rather high temperature, $T = 1$, the degree of classical correlations is larger than quantum correlations, this is actually a property
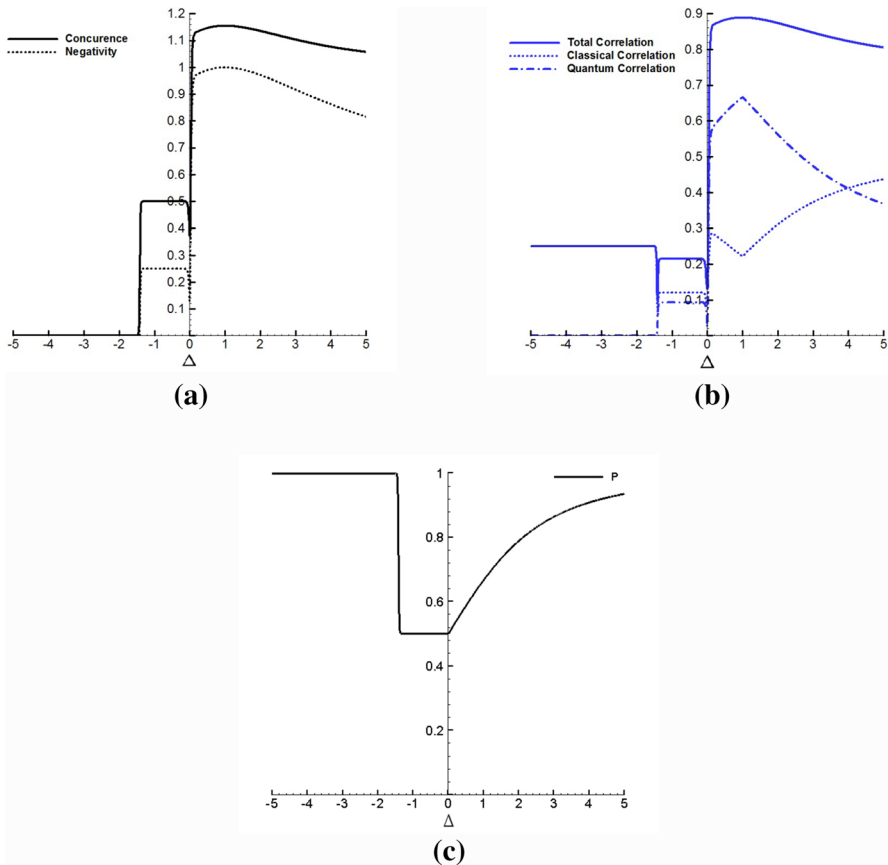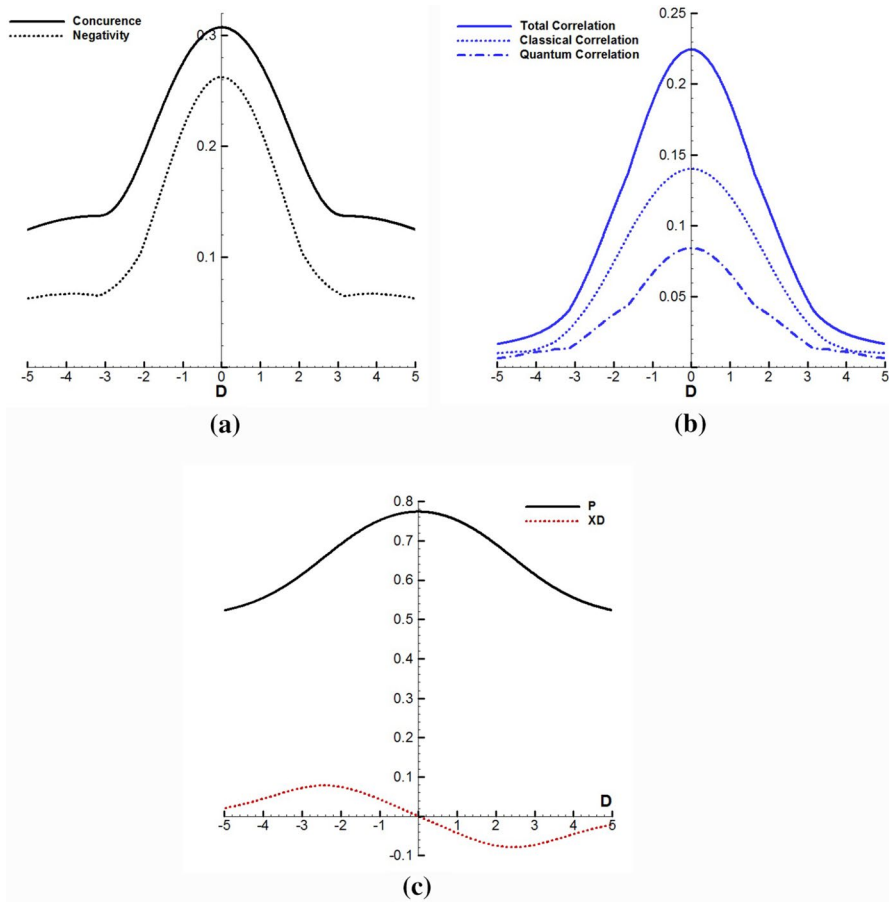

Fig. 4 (Color figure online) Generalized concurrence (solid), negativity (dotted) (**a**), total correlation (solid), classical correlation (dotted) and quantum correlation (dashed) (**b**) and particle number (**c**) versus Δ for $J = 1$ and $D = 1$ at $T = 0.01$

Fig. 5 (Color figure online) Generalized concurrence (solid), negativity (dotted) (**a**), total correlation(solid), classical correlation (dotted) and quantum correlation (dashed) (**b**) and particle number (solid) and particle susceptibility (dotted) (**c**) versus D for $J = 1$ and $\Delta = 2$ with $N = 2$ at $T = 1$

of classical physics. That is, as temperature increases, the system behaves classically. In addition, comparing with the low-temperature cases, we see that the amount of entanglement and correlation functions decreases by increasing the temperature of the system. The results for $J = 1$, $D = 0$ and $T = 1$ are depicted in Fig. 6. As in the previous case, no critical point occurs and the variation of functions are more smooth with respect to the low-temperature cases. Moreover, the value of the classical correlations is everywhere larger than the quantum correlations. In Fig. 7, pairwise correlation functions are plotted as a function of T for $D = 1$ (Fig. 7a) and $D = -1$ (Fig. 7b) when $J = 1$. From the figure, it is clear that the correlation functions tend to zero at large temperatures. If we compare the behavior of the correlation functions for two cases, we observe that for $T < 1$ when $D = 1$, the amount of classical correlations is larger than the quantum
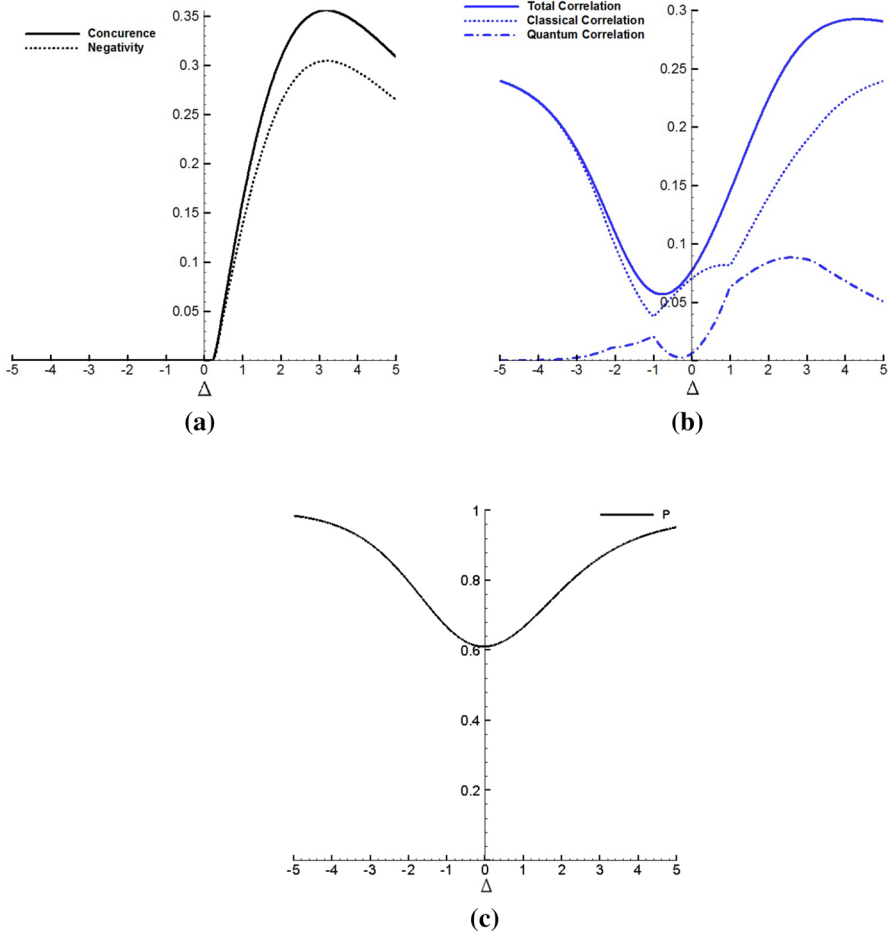
Fig. 6 (Color figure online) Generalized concurrence (solid), negativity (dotted) (**a**), total correlation (solid), classical correlation (dotted) and quantum correlation (dashed) (**b**) and particle number (**c**) versus Δ for $J = 1$ and $D = 0$ at $T = 1$

correlations, while for $D = -1$, the classical correlations are smaller than quantum correlations. For $T > 1$, the classical correlations are larger than the quantum correlations for both values of D.

5 Three-Particle System

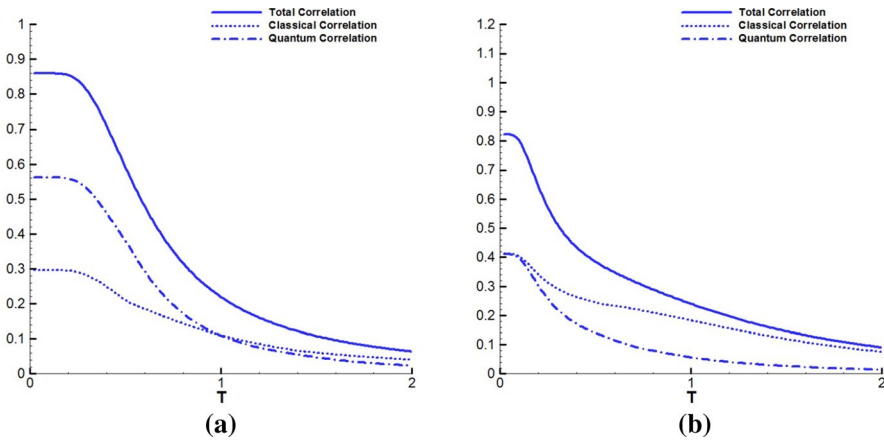Here, we consider the case of three-spin-1 chain ($N = 3$). The Hamiltonian of this system can be written as follows:

Fig. 7 (Color figure online) Total correlation (solid), classical correlation (dotted) and quantum correlation (dashed) versus T for $D = 1$ (**a**) and $D = -1$ (**b**) with $J = 1$ and $N = 2$

$$H_3 = J\left(S_1^x S_2^x + S_1^y S_2^y + S_2^x S_3^x + S_2^y S_3^y + S_3^x S_1^x + S_3^y S_1^y + \Delta(S_1^z S_2^z + S_2^z S_3^z + S_3^z S_1^z)\right)$$
$$- D((S_1^z)^2 - (S_2^z)^2 + (S_3^z)^2)$$

$$(14)$$

Like the two-particle case, we obtain the eigenvalues of the Hamiltonian matrix (14) and calculate thermal density matrix to derive pairwise correlations, entanglement measures and particle number. Here, we assume the bipartition $3 \otimes 9$; that is, we perform the calculations for the correlation between one particle and the remaining two particles.

Figure 8 displays the behavior of the entanglement measures, correlation functions and particle number, for anti-ferromagnetic case, $J = 1$, at $T = 0.02$. From the figure, it is clear that sudden jumps appear at $D = \pm 2.56$. For large positive and negative values of D, all functions are constants with different values. For $D < -2.56$, the negativity is larger than the concurrence. Depending on D parameter, classical correlations are smaller or larger than quantum correlations in the interval between the two critical points, that is, $-2.56 < D < 2.56$, in contrast to the two-particle case. For outside of this range, classical correlations are larger than quantum correlations similar to the two-particle case. For $J = -1$, two critical points appear at $D = -2.5$ and $D = 3.54$. In the interval $-2.5 < D < 3.54$, the values of entanglement and quantum correlations are zero while classical correlations and particle number take their maximum values. Outside the range, $D < -2.5$ and $D > 3.54$, classical correlations are also larger than quantum correlations (see Fig. 9). This behavior is similar to the two-particle case in Fig. 2.

Figure 10 shows the effect of the Δ parameter on the system for $J = 1$ and $D = 0$ at low temperature. We observe that a critical point is found at $\Delta = -0.5$. For large positive and negative values of Δ, all the studied functions tend to constant but different values. Unlike the case of a two-particle system (Fig. 3), here, quantum correlations are larger than classical correlations for each value of Δ
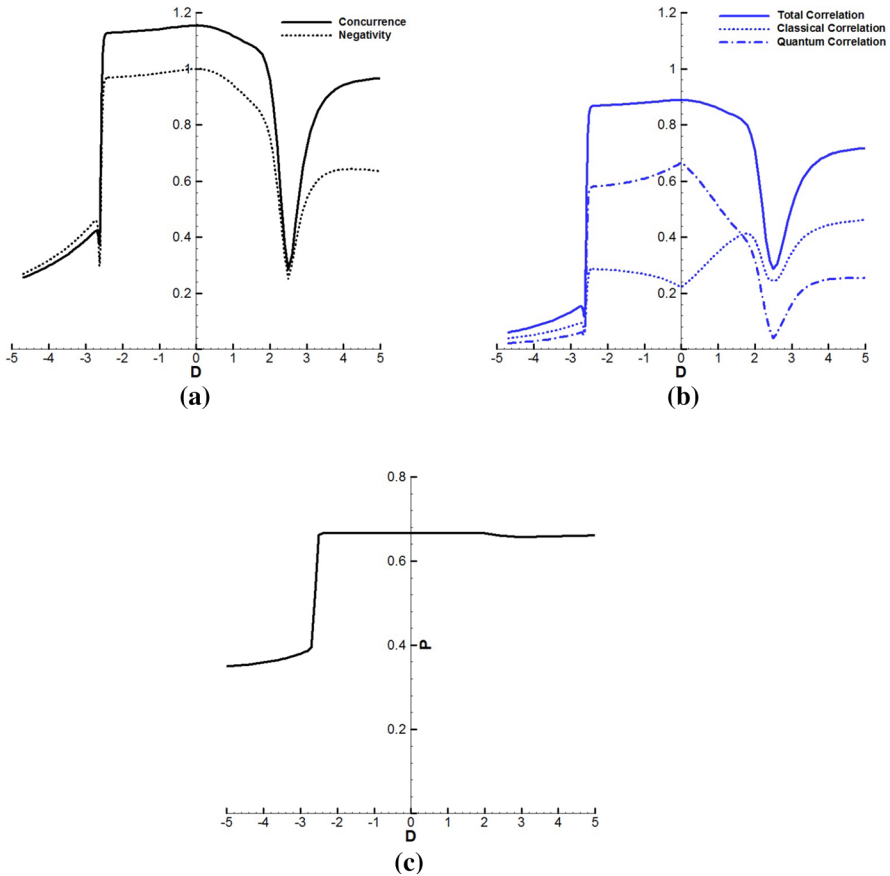
Fig. 8 (Color figure online) Generalized concurrence (solid), negativity (dotted) (**a**), total correlation (solid), classical correlation (dotted) and quantum correlation (dashed) (**b**) and particle number (**c**) versus D for $J = 1$, $\Delta = 2$ and $N = 3$ at $T = 0.02$

larger than the critical point. On the other hand, for each value of Δ smaller than the critical point, the system behaves similar to the two-particle case.

Now, we discuss the case $D = 1$ as the results are depicted in Fig. 11. If we compare Figs. 10 and 11, we see that the properties of the physical system are similar for both of D values except for the $D = 1$ case that we have two quantum critical points $\Delta = -0.8$ and $\Delta = -0.2$. Figure 12 shows the results corresponding to pairwise correlations, entanglement measures and particle number for $J = -1$ and $D = 0$ at low temperature. A comparison between Figs. 10 and 12 reveals that due to the critical point at $\Delta = 1$, two figures are not completely symmetric to each other. Although as $\Delta \to \pm\infty$, the behavior of the system with $J = -1$ is similar to the results we obtained for the system with $J = 1$ as $\Delta \to \mp\infty$, but the critical points are not symmetrical.

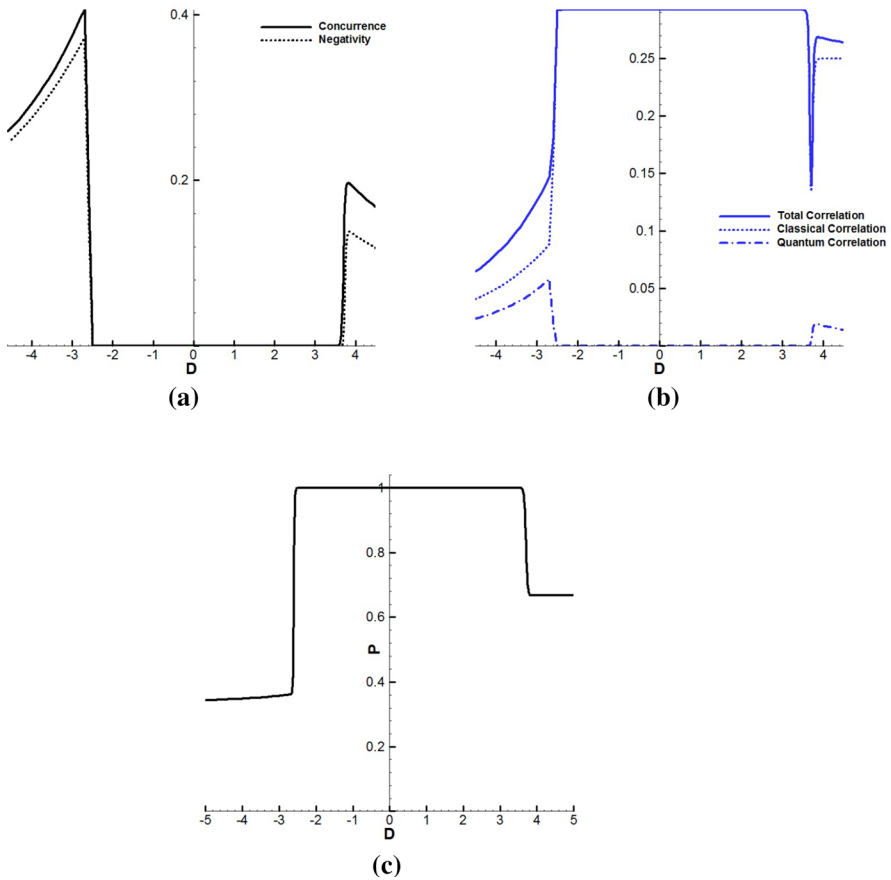**Fig. 9** (Color figure online) Generalized concurrence (solid), negativity (dotted) (**a**), total correlation (solid), classical correlation (dotted) and quantum correlation (dashed) (**b**) and particle number (**c**) versus D for $J = -1$, $\Delta = 2$ and $N = 3$ at $T = 0.02$

Similar results are obtained for $J = -1$ and $D = 1$ cases, except for two critical points, $\Delta = 0.7$ and $\Delta = 1$ appearing when $D = 1$, as depicted in Fig. 13. Now, we investigate how the system is affected by temperature when $J = 1$ and $N = 3$. From Fig. 14a, for $D = 1$ and $T < 0.38$, the quantum correlations are larger than the classical correlations and for $T > 0.38$, the classical correlations are larger than the quantum correlations. For $D = -1$ (Fig. 14b), when $T < 1$, the quantum correlations are larger than the classical correlations. On the other hand, for $T > 1$, the classical correlations are larger than the quantum correlations for both values of D.
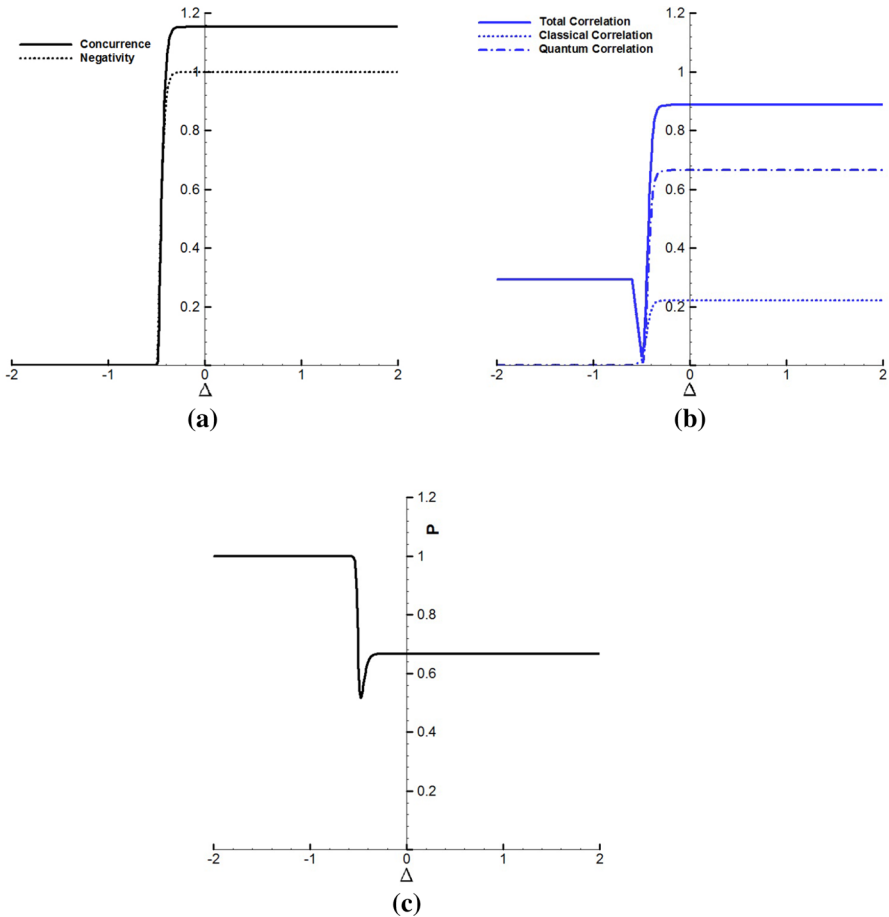
Fig. 10 (Color figure online) Generalized concurrence (solid), negativity (dotted) (**a**), total correlation (solid), classical correlation (dotted) and quantum correlation (dashed) (**b**) and particle number (**c**) versus Δ for $J = 1$, $D = 0$ and $N = 3$ at $T = 0.02$

6 Conclusion

In summary, we have discussed thermal pairwise correlations, quantified by classical, quantum and total amount of correlations as well as the entanglement measures, that is, the generalized concurrence and the negativity, and also the particle number and the particle susceptibility functions. It is found out that the generalized concurrence, the negativity and pairwise correlations can be used to determine QPTs. We have shown that for only finite, but low temperatures, the system undergoes a QPT. By increasing the temperature, QPTs no longer occur. At low temperatures, depending on the parameters of the Hamiltonian, the quantum correlations are larger or smaller than the classical correlations. Yet at high temperatures, the classical
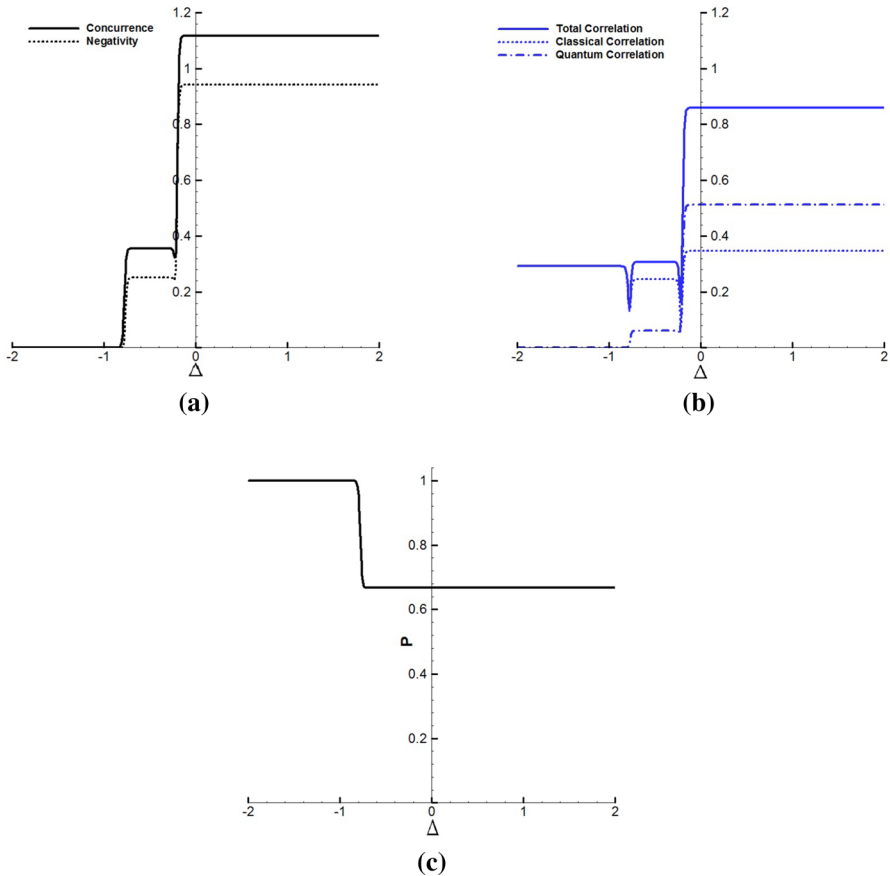
Fig. 11 (Color figure online) Generalized concurrence (solid), negativity (dotted) (**a**), total correlation (solid), classical correlation (dotted) and quantum correlation (dashed) (**b**) and particle number (**c**) versus Δ for $J = 1$, $D = 1$ and $N = 3$ at $T = 0.02$

correlations are generally larger than the quantum correlations. Unlike to the two-particle case, in three-particle system, for $J = 1$ and in the parameter space D, the amount of the negativity measure is larger than the concurrence measure. Also, depending on the D parameter, quantum correlations are larger or smaller than classical correlations. For the two-particle system, there is a symmetry with respect to J with the same D value while for the three-particle case, the system has no symmetry with respect to J with the same D. For the $D = 0$ case, we have one quantum critical point whereas for the $D = 1$ case, the system undergoes two QPTs for both the two- and the three-particle cases.
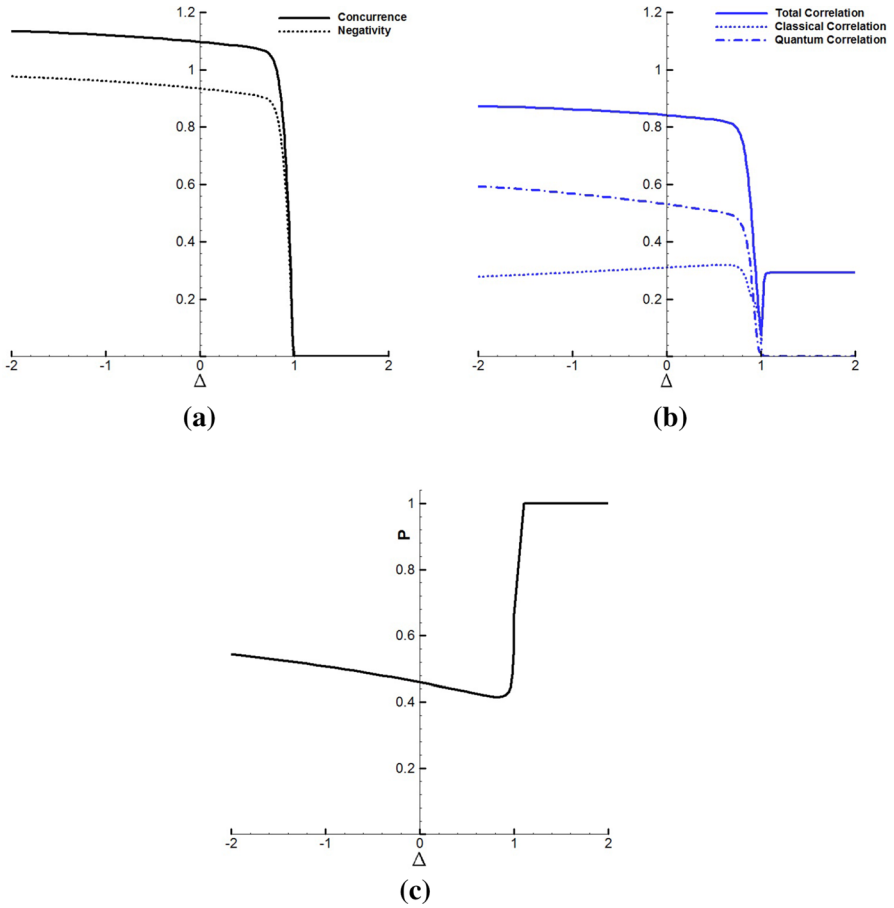
Fig. 12 (Color figure online) Generalized concurrence (solid), negativity (dotted) (**a**), total correlation (solid), classical correlation (dotted) and quantum correlation (dashed) (**b**) and particle number (**c**) versus Δ for $J = -1$, $D = 0$ and $N = 3$ at $T = 0.02$
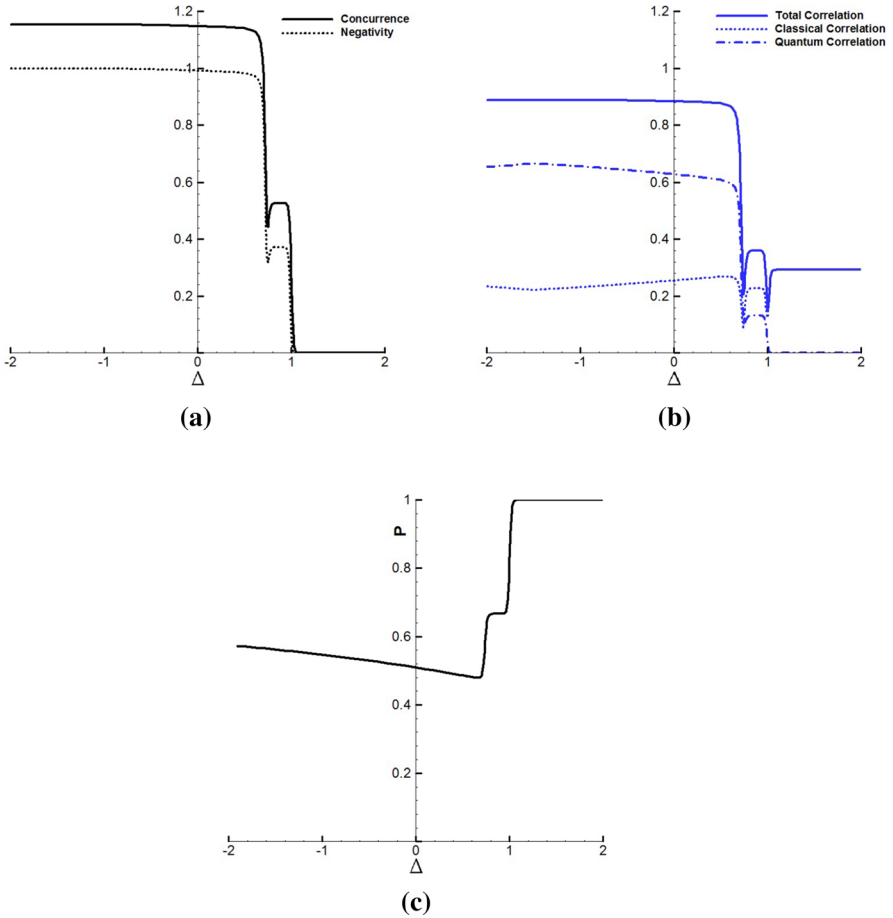
(a)

(b)

(c)

Fig. 13 (Color figure online) Generalized concurrence (solid), negativity (dotted) (**a**), total correlation (solid), classical correlation (dotted) and quantum correlation (dashed) (**b**) and particle number (**c**) versus Δ for $J = -1$, $D = 1$ and $N = 3$ at $T = 0.02$
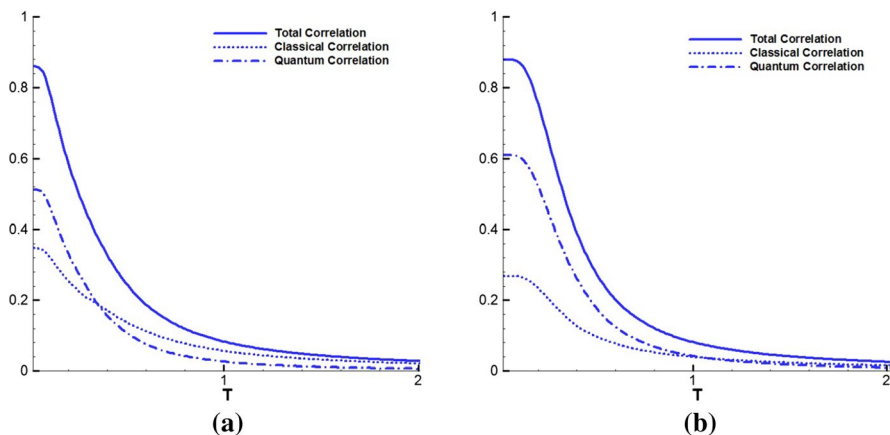
Fig. 14 (Color figure online) Total correlation (solid), classical correlation (dotted) and quantum correlation (dashed) versus T for $D = 1$ (**a**) and $D = -1$ (**b**) with $J = 1$ and $N = 3$

References

1. M. Nielsen, I. Chuang, *Quantum Computation and Quantum Information, Cambridge Series on Information and the Natural Sciences* (Cambridge University Press, Cambridge, 2000).
2. M.C. Arnesen, S. Bose, V. Vedral, Phys. Rev. Lett. **87**, 017901 (2001)
3. X. Wang, Phys. Rev. A **64**, 012313 (2001)
4. X. Wang, Phys. Lett. A **281**, 101 (2001)
5. G.L. Kamta, A.F. Starace, Phys. Rev. Lett. **88**, 107901 (2002)
6. T.J. Osborne, M.A. Nielsen, Phys. Rev. A **66**, 032110 (2002)
7. M. Asoudeh, V. Karimipour, Phys. Rev. A **70**, 052307 (2004)
8. M. Asoudeh, V. Karimipour, Phys. Rev. A **71**, 022308 (2005)
9. N. Canosa, R. Rossignoli, Phys. Rev. A **69**, 052306 (2004)
10. G. Najarbashi, L. Balazadeh, A. Tavana, Int. J. Theor. Phys. **57**, 95 (2018)
11. L. Balazadeh, G. Najarbashi, A. Tavana, Sci. Rep. **8**, 17789 (2018)
12. K.M. O'Connor, W.K. Wootters, Phys. Rev. A **63**, 0520302 (2001)
13. D. A. Meyer, N. R. Wallach, quant-ph/0108104
14. T. J. Osborne, M. A. Nielsen, quant-ph/ 0202162
15. A. Osterloh, L. Amico, G. Falci, R. Fazio, Nature **416**, 608 (2002)
16. S. Sachdev, *Quantum Phase Transitions* (Cambridge University Press, Cambridge, 2000)
17. H. Olivier, W.H. Zurek, Phys. Rev. Lett. **88**, 017901 (2001)
18. J. Oppenheim, M. Horodecki, P. Horodecki, R. Horodecki, Phys. Rev. Lett. **89**, 180402 (2002)
19. L. Henderson, V. Vedral, J. Phys. A **34**, 6899 (2001)
20. L.-A. Wu, M.S. Sarandy, D.A. Lidar, Phys. Rev. Lett. **93**, 250404 (2004)
21. M.S. Sarandy, Phys. Rev. A **80**, 022108 (2009)
22. K. Modi, A. Brodutch, H. Cable, T. Paterek, V. Vedral, Rev. Mod. Phys. **84**, 1655 (2012)
23. T. Werlang, G.A.P. Ribeiro, G. Rigolin, Int. J. Modern Phys. B **27**(1–3), 1345032 (2013)
24. M.S. Sarandy, T.R.D. Oliveira, Int. J. Modern Phys. B **27**(1—-3), 1345030 (2013)
25. F.D.M. Haldane, Phys. Rev. Lett. **50**, 1153 (1983)
26. J. Ren, G.H. Liu, W.L. You, J. Phys. Condens. Matter **27**, 105602 (2015)
27. J. Chakhalian, J.W. Freeland, A.J. Millis, C. Panagopoulos, J.M. Rondinelli, Rev. Modern Phys. **86**, 1189 (2014)
28. Y.C. Tzeng, M.F. Yang, Phys. Rev. A **77**, 012311 (2008)
29. T. Zhou, J. Cui, G.L. Long, Phys. Rev. A **84**, 062105 (2011)
30. A. Uhlmann, Phys. Rev. A **62**, 032307 (2000)
31. P. Rungta, V. Buzek, C.M. Caves, M. Hillery, G.J. Milburn, Phys. Rev. A **64**, 042315 (2001)

32. K. Audenaert, F. Verstraete, D. Moor, Phys. Rev. A **64**, 052304 (2001)
33. S. Albeverio, S.M. Fei, J. Opt. B Quantum Semiclass. Opt. **3**, 1 (2001)
34. H. Fan, K. Matsumoto, H. Imai, J. Phys. A Math. Gen. **36**, 4151 (2003)
35. P. Badziag, P. Deuar, M. Horodecki, P. Horodecki, R. Horodecki, quant-ph/0107147 (2001)
36. Y.Q. Li, G.Q. Zhu, Front. Phys. China **3**(3), 250–257 (2008)
37. S.J. Akhtarshenas, J. Phys. A Math. Gen. **38**, 6777–6784 (2005)
38. A. Peres, Phys. Rev. Lett. **76**, 1413–1416 (1996)
39. G. Vidal, R.F. Werner, Phys. Rev. A **65**, 032314 (2002)
40. T. Laustsen, F. Verstraete, S.J. van Enk, Quantum Inf. Comput. **3**, 64 (2003)
41. V.S. Abgaryan, N.S. Ananikian, L.N. Ananikyan, A.N. Kocharian, Phys. Scr. **83**, 055702 (2011)
42. S. Hill, W.K. Wootters, Phys. Rev. Lett. **78**, 5022 (1997)
43. W.K. Wootters, Phys. Rev. Lett. **80**, 2245 (1998)
44. W.K. Wootters, Quantum Inf. Comput. **1**, 27–44 (2001)
45. X.-H. Gao, A. Sergio, K. Chen, S.-M. Fei, X.-Q. Li-Jost, Front. Coumput. Sci. China **2**(2), 114–128 (2008)
46. K. Chen, S. Albeverio, S.-M. Fei, Phys. Rev. Lett. **95**, 210501 (2005)
47. M. Horodecki, P. Horodecki, R. Horodecki, Phys. Lett. A **223**, 1 (1996)